

## Flow around Clark-Y airfoil: Summary of EFD benchmark data and comparison with IIHR EFD data and CFD solution

**Nobuaki Sakamoto, Colin J. Johnson, Stuart Brezinski, Marian V. Muste and Frederick Stern  
IIHR-Hydroscience&Engineering, The University of Iowa**

1. EFD benchmark data

[1] JACOBS E.N., STACK J., AND PINKERTON R.M., 1930 Airfoil pressure distribution investigation in the variable density wind tunnel, Langley Memorial Aeronautical Laboratory Report No. 353

[2] MARCHMAN J.F. AND WERME T.D., 1984 Clark-Y airfoil performance at low Reynolds numbers, In: proc. AIAA 22<sup>nd</sup> Aerospace Science Meeting, Jan. 9-12, Reno, Nevada, U.S.A.

[3] SILVERSTEN A., 1934, Scale effect on Clark-Y airfoil characteristics from NACA full-scale wind-tunnel tests, Langley Memorial Aeronautical Laboratory Report No. 502

[4] ZIMMERMAN C.H., Characteristics of Clark-Y airfoils of small aspect ratios, 1932, Langley Memorial Aeronautical Laboratory Report No. 431

The summary of EFD benchmark data is given in Table 1.

Table 1 Summary of EFD benchmark data

Reference	[1]	[2]		[3]	[4]
Digitized data	$C_p$ and $C_L$	$C_p$ , $C_L$ and $C_D$		$C_L$ and $C_D$	$C_L$ and $C_D$
AR*	7.2	5.75		6	0.5, 0.75, 1, 1.25, 1.5, 2, 3, 6
Re**	3.56e5	$C_p$	7.5e4	1.12e6, 1.55e6, 2.06e6, 2.81e6, 3.19e6, 3.59e6	8.6e5
		$C_L$ , $C_D$	5e4, 7.5e4, 1e5, 2e5, 6.7e6		
$\alpha$ (deg)***	1, 4, 7, 10,13, 17, 20	$C_p$	0, 4, 6, 8, 12, 14	0, 1, 2, 3, 4, 5, 6, 7, 8, 9, 10, 11, 12, 13, 14, 15, 16, 17, 18, 19, 20, 21, 22, 23	0, 10, 15, 20, 25, 30, 35, 39, 40, 42, 50, 60
		$C_L$ , $C_D$	0, 4, 6, 8, 12, 14		
Wingtip		End plates		Wing cross section	Rectangular

\*: Aspect ratio, \*\*: Reynolds number, \*\*\*: Angle of attack

2. Trend of each data set

2.1 Reference [1]

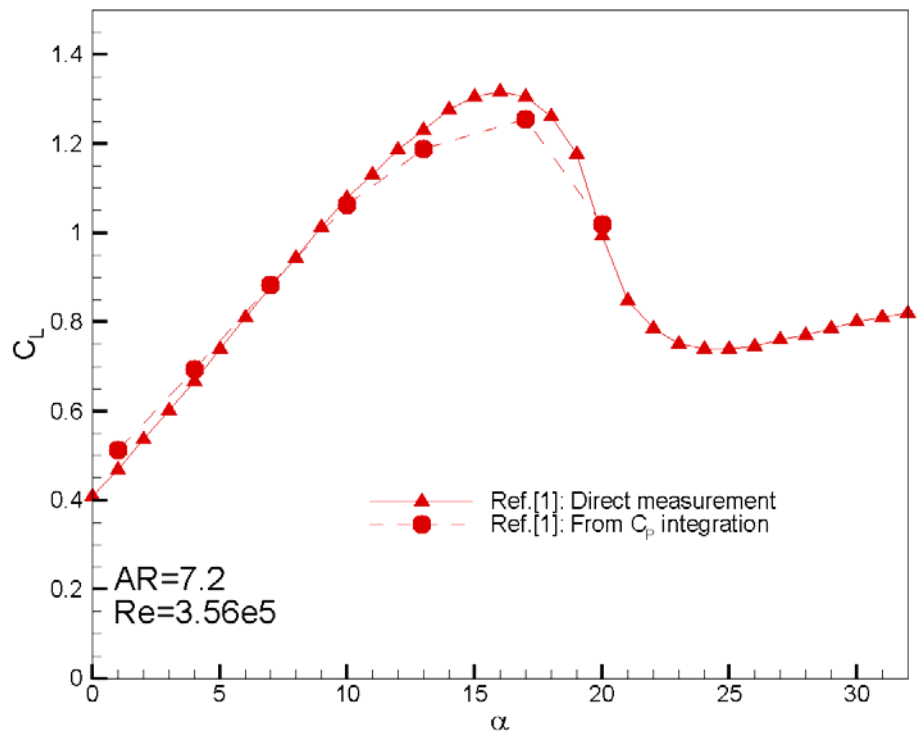


Fig. 1 Trend of  $C_L$  in Reference [1]

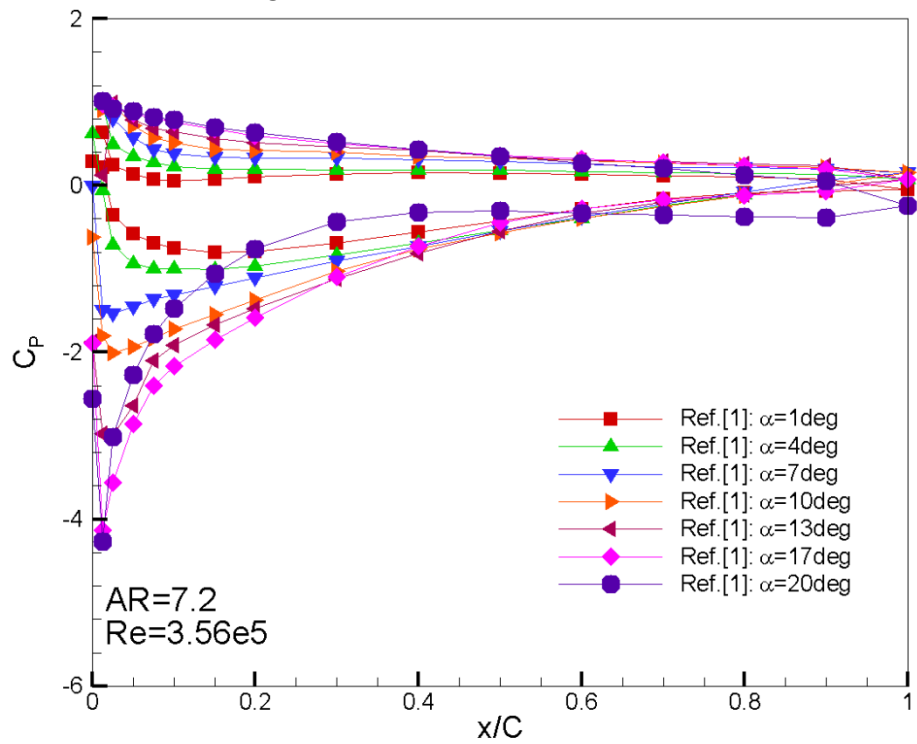


Fig. 2 Trend of  $C_p$  in Reference [1]

2.2 Reference [2]

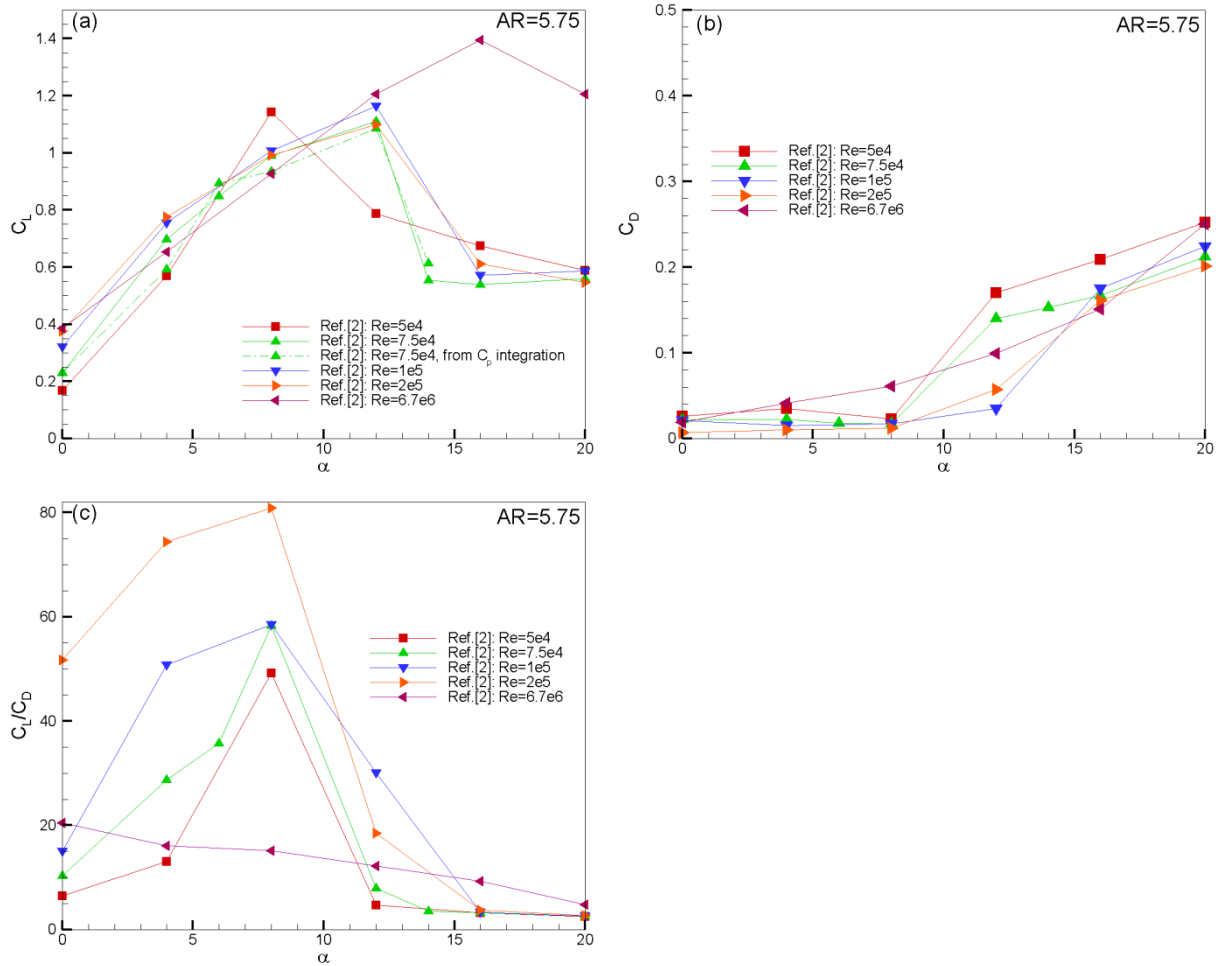


Fig. 3 Trend of  $C_L$ ,  $C_D$ , and  $C_L/C_D$  with variations of  $Re$  in Reference [2]  
 (a)  $C_L$  vs  $\alpha$ , (b)  $C_D$  vs  $\alpha$ , (c)  $C_L/C_D$  vs  $\alpha$

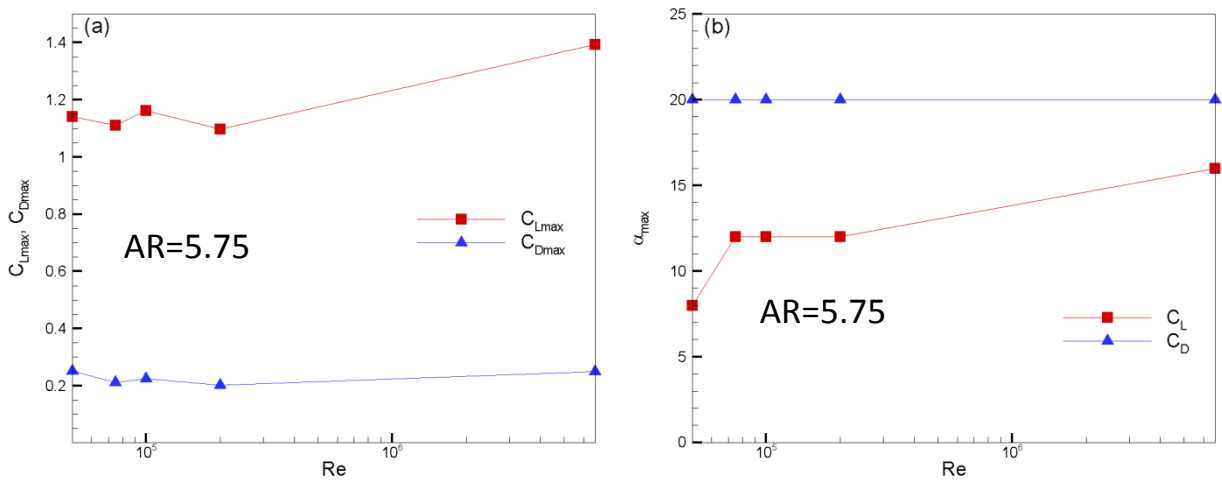


Fig. 4 Re dependency of  $C_{Lmax}$ ,  $C_{Dmax}$  and  $\alpha_{max}$  in Reference [2]: (a)  $C_{Lmax}$ ,  $C_{Dmax}$  vs  $Re$ , (b)  $\alpha_{max}$  vs  $Re$

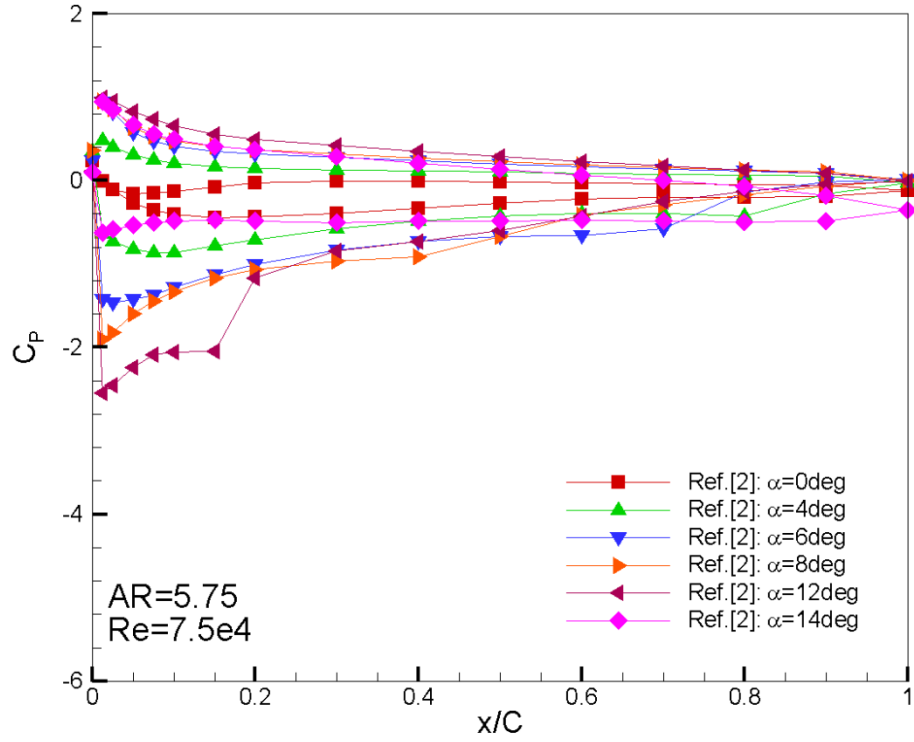


Fig. 5 Trend of  $C_p$  in Reference [2]

2.3 Reference [3]

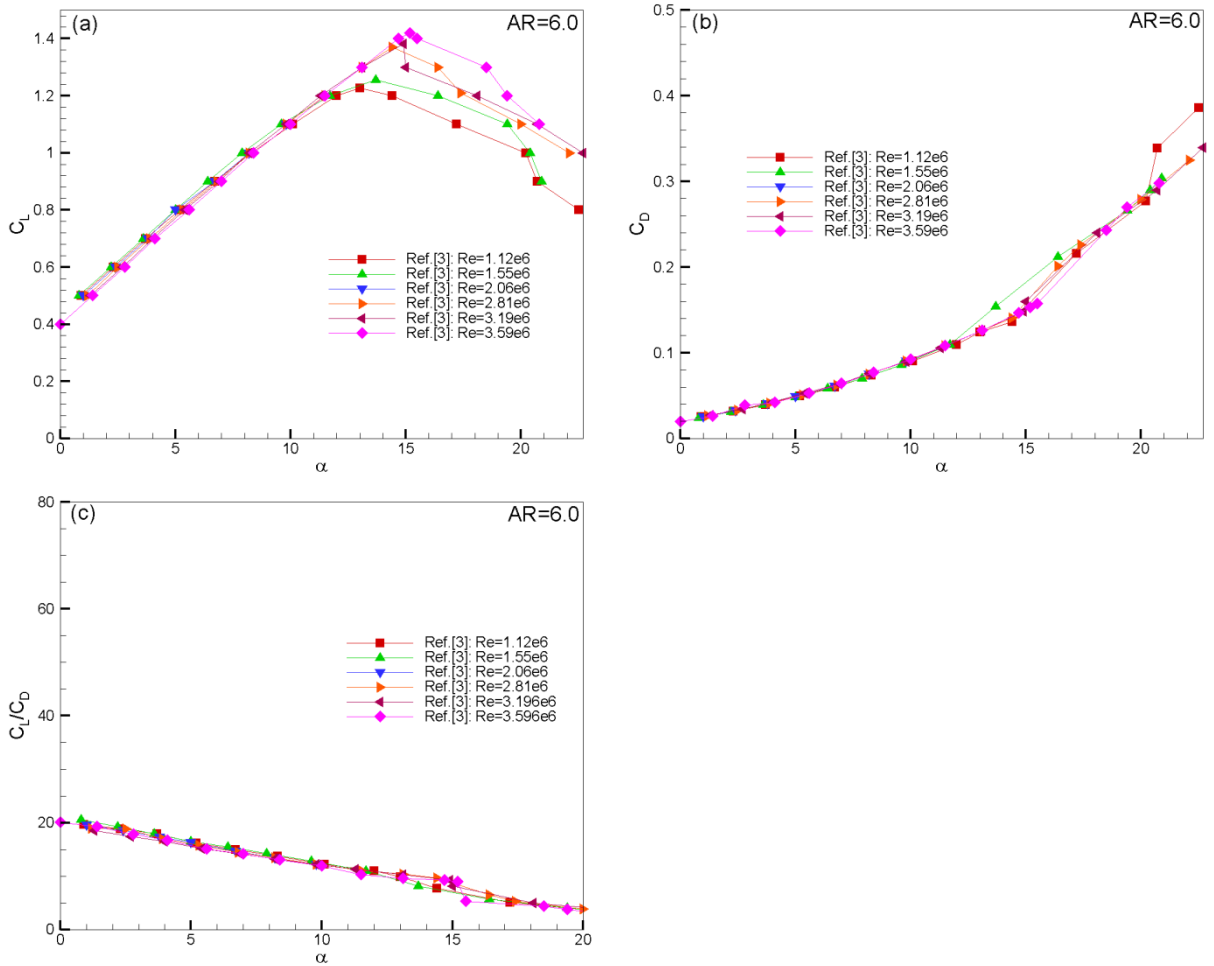


Fig. 6 Trend of  $C_L$ ,  $C_D$ , and  $C_L/C_D$  with variations of  $Re$  in Reference [3]  
 (a)  $C_L$  vs  $\alpha$ , (b)  $C_D$  vs  $\alpha$ , (c)  $C_L/C_D$  vs  $\alpha$

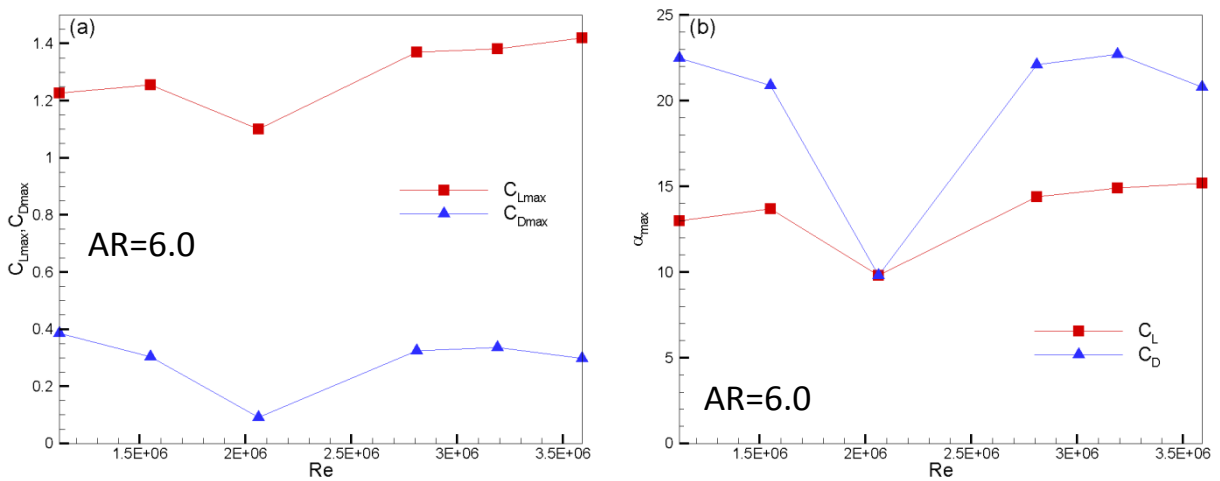


Fig. 7  $Re$  dependency of  $C_{Lmax}$  and  $\alpha_{max}$  for  $C_L$  in Reference [3]: (a)  $C_{Lmax}$  vs  $Re$ , (b)  $\alpha_{max}$  vs  $Re$

2.4 Reference [4]

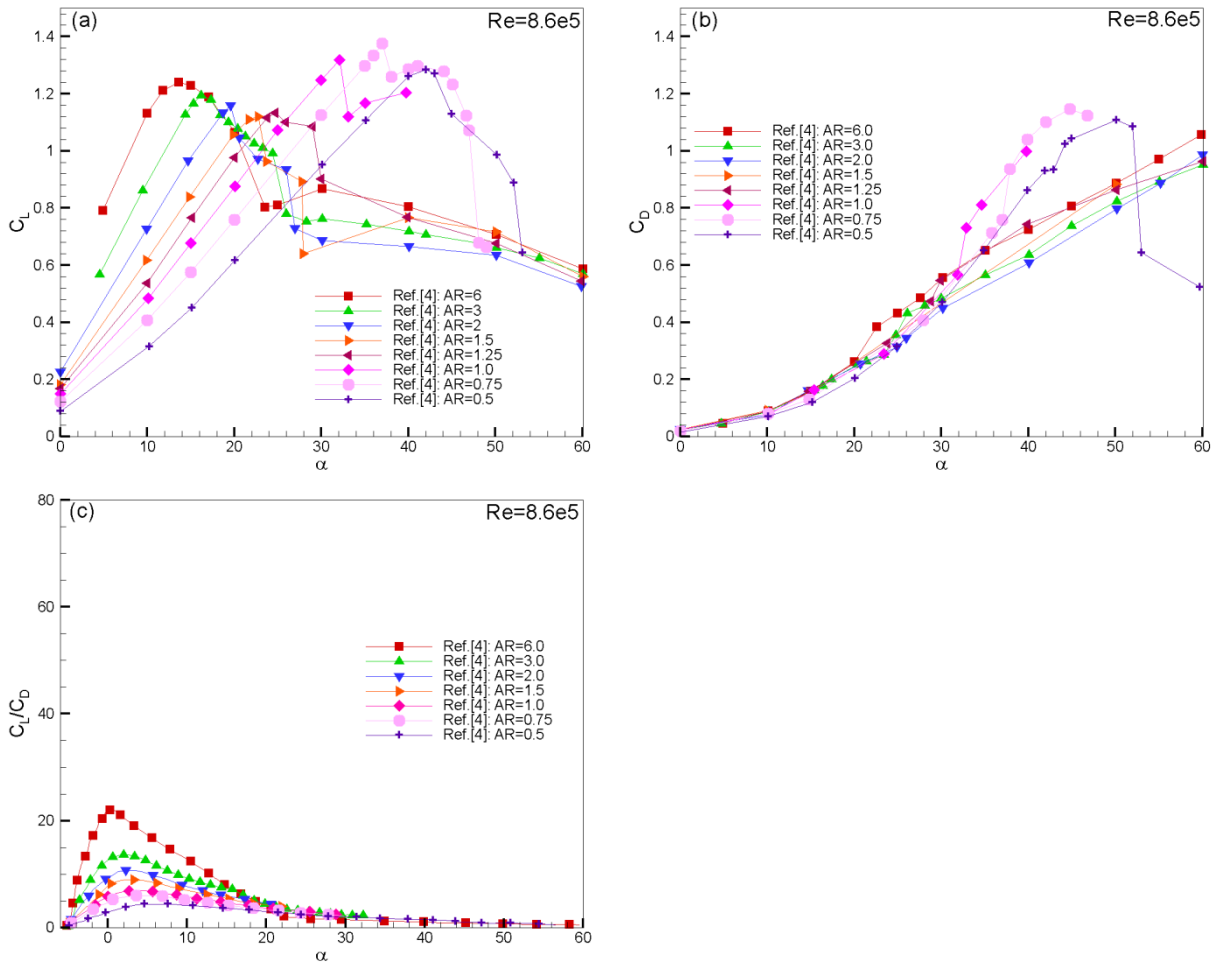


Fig. 8 Trend of  $C_L$ ,  $C_D$ , and  $C_L/C_D$  with variations of AR in Reference [4]  
 (a)  $C_L$  vs  $\alpha$ , (b)  $C_D$  vs  $\alpha$ , (c)  $C_L/C_D$  vs  $\alpha$

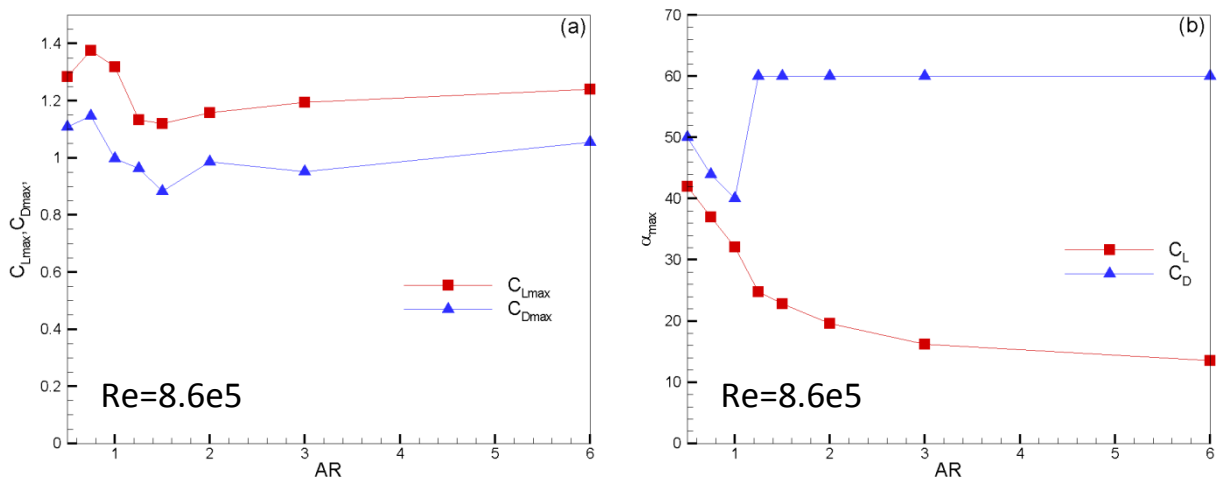


Fig. 9 Aspect ratio dependency of  $C_{Lmax}$  and  $\alpha_{max}$  for  $C_L$  in Reference [4]: (a)  $C_{Lmax}$  vs AR, (b)  $\alpha_{max}$  vs AR

3. Comparison between the reference experimental data

3.1  $C_L$  vs  $\alpha$  with largest AR

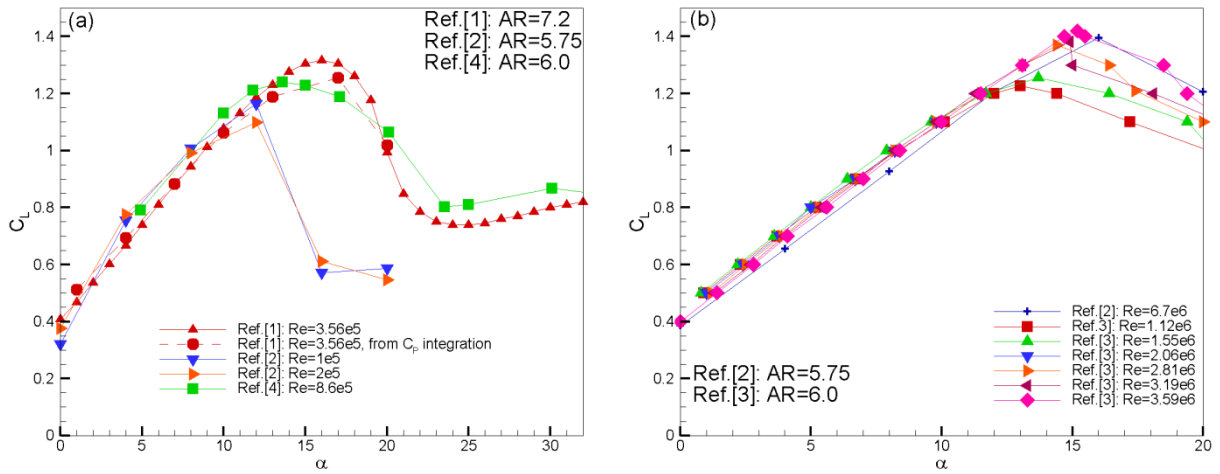


Fig. 10  $C_L$  vs  $\alpha$  with largest AR: (a)  $Re=O(10^5)$ , (b)  $Re=O(10^6)$

3.2  $C_D$  vs  $\alpha$  with largest AR

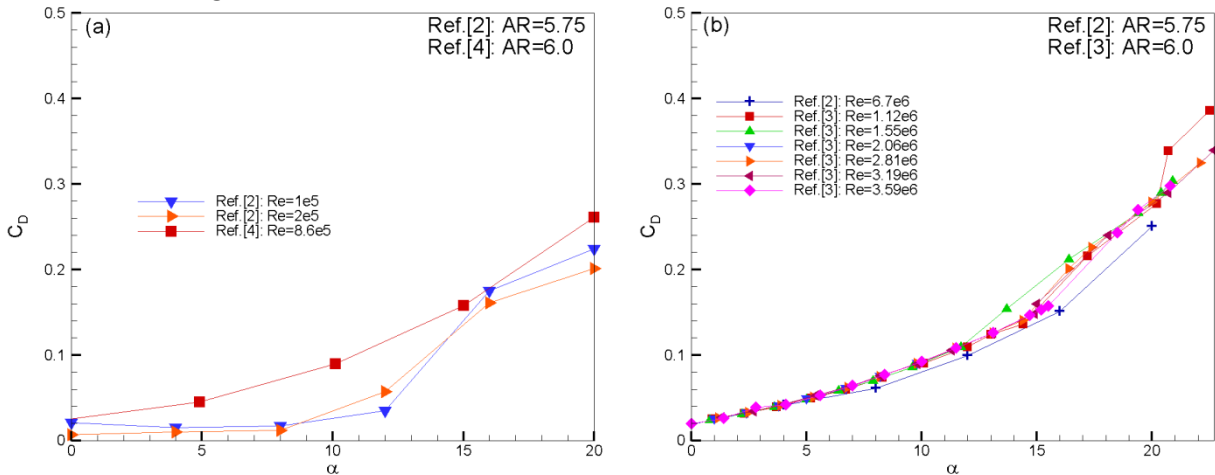


Fig. 11  $C_D$  vs  $\alpha$  with largest AR: (a)  $Re=O(10^5)$ , (b)  $Re=O(10^6)$

3.3  $C_L/C_D$  vs  $\alpha$  with largest AR

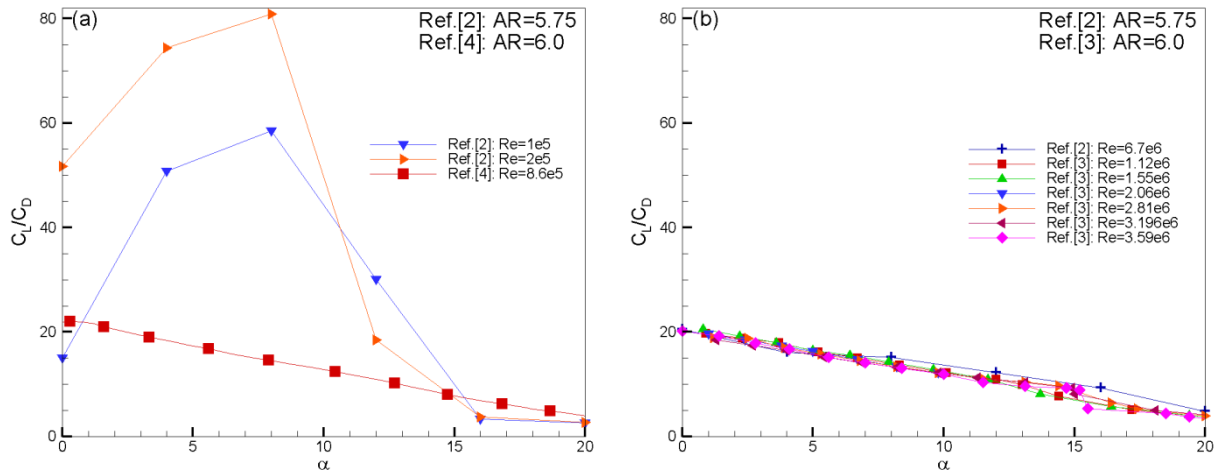


Fig. 12  $C_D$  vs  $\alpha$  with largest AR: (a)  $Re=O(10^5)$ , (b)  $Re=O(10^6)$

3.5  $C_{Lmax}$ ,  $C_{Dmax}$  and  $\alpha_{max}$  with largest AR

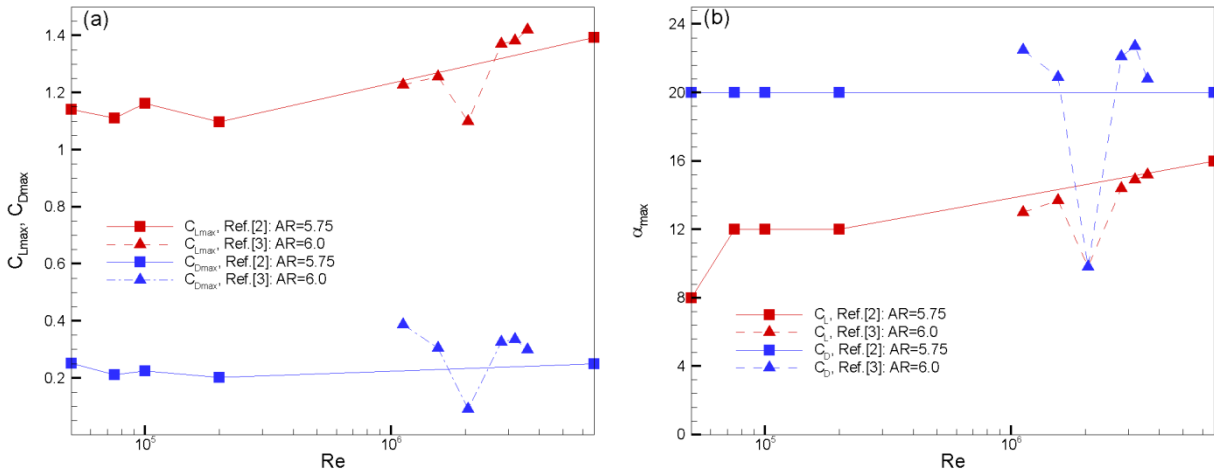


Fig. 13  $Re$  dependency for  $C_{Lmax}$ ,  $C_{Dmax}$  and  $\alpha_{max}$ : (a)  $C_{Lmax}$ ,  $C_{Dmax}$  vs  $Re$ , (b)  $\alpha_{max}$  vs  $Re$



3.4  $C_p$  with largest AR

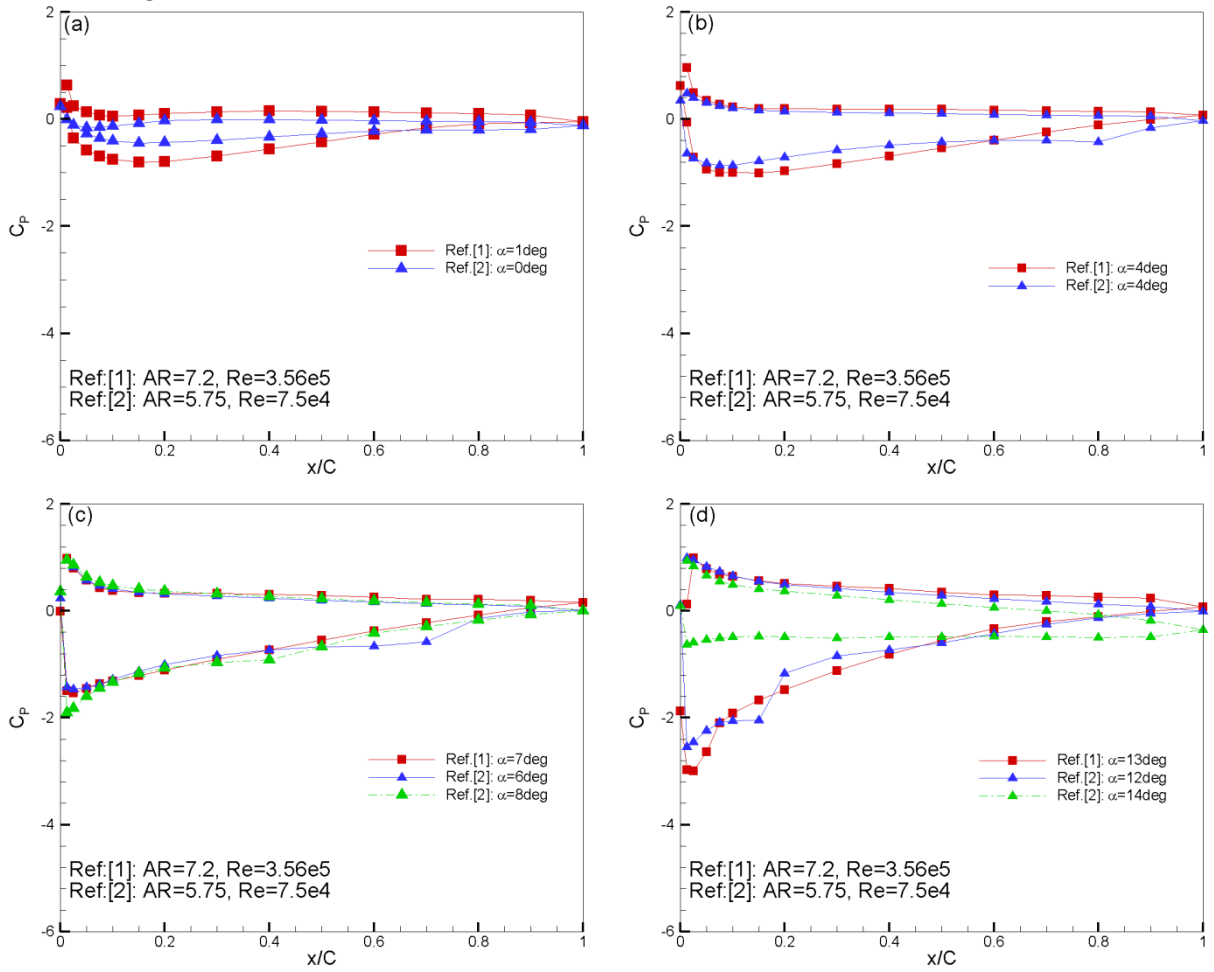


Fig. 14  $C_p$  distribution with largest AR: (a)  $\alpha \approx 0^\circ$ , (b)  $\alpha \approx 4^\circ$ , (c)  $\alpha \approx 7^\circ$ , (d)  $\alpha \approx 13^\circ$

4. Comparison with Flowlab simulation results

4.1  $C_L$  vs  $\alpha$

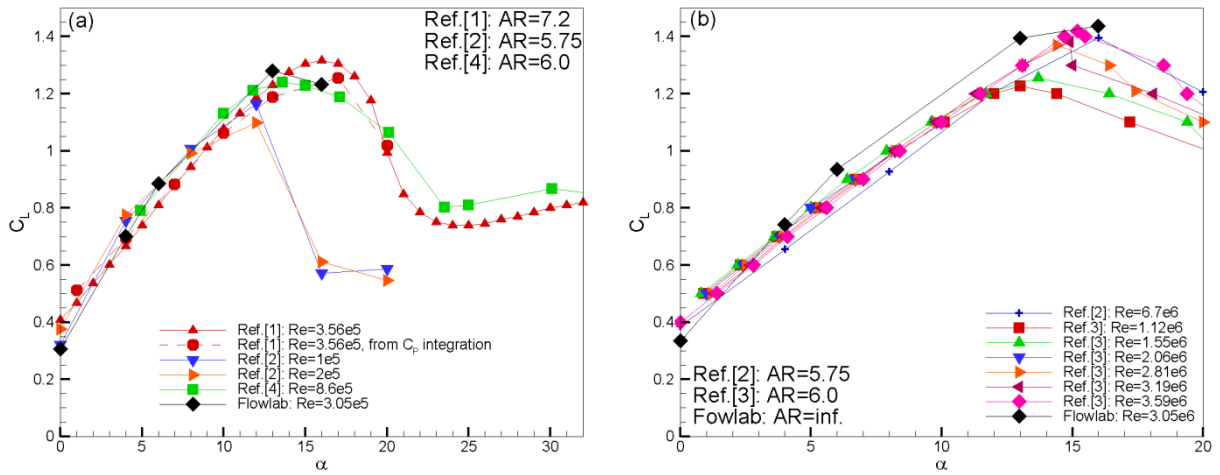


Fig. 15  $C_L$  vs  $\alpha$  with largest AR, Flowlab solutions added: (a)  $Re=O(10^5)$ , (b)  $Re=O(10^6)$

4.2  $C_D$  vs  $\alpha$

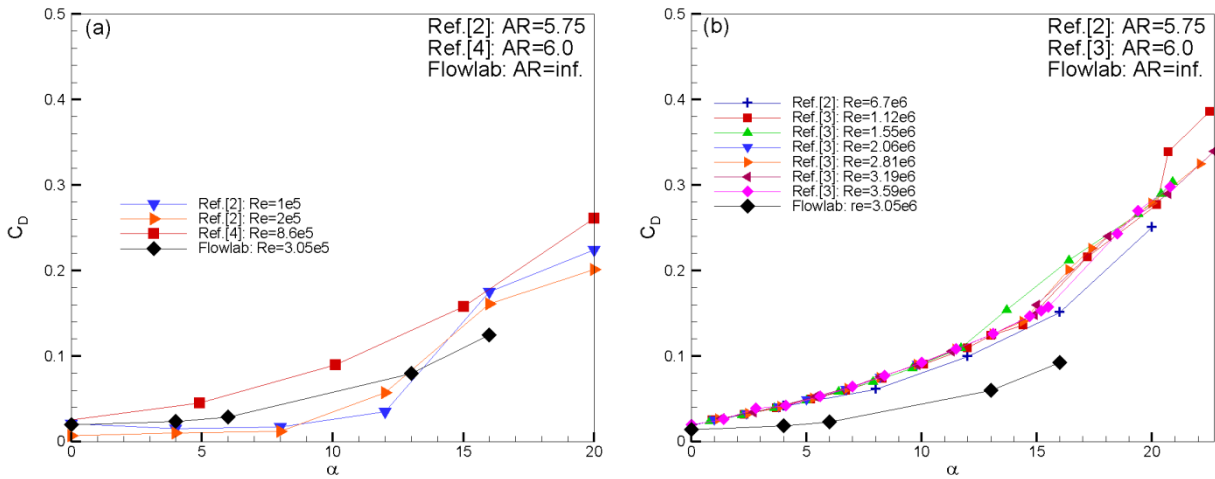


Fig. 16  $C_D$  vs  $\alpha$  with largest AR, Flowlab solutions added: (a)  $Re=O(10^5)$ , (b)  $Re=O(10^6)$

4.3  $C_L/C_D$  vs  $\alpha$

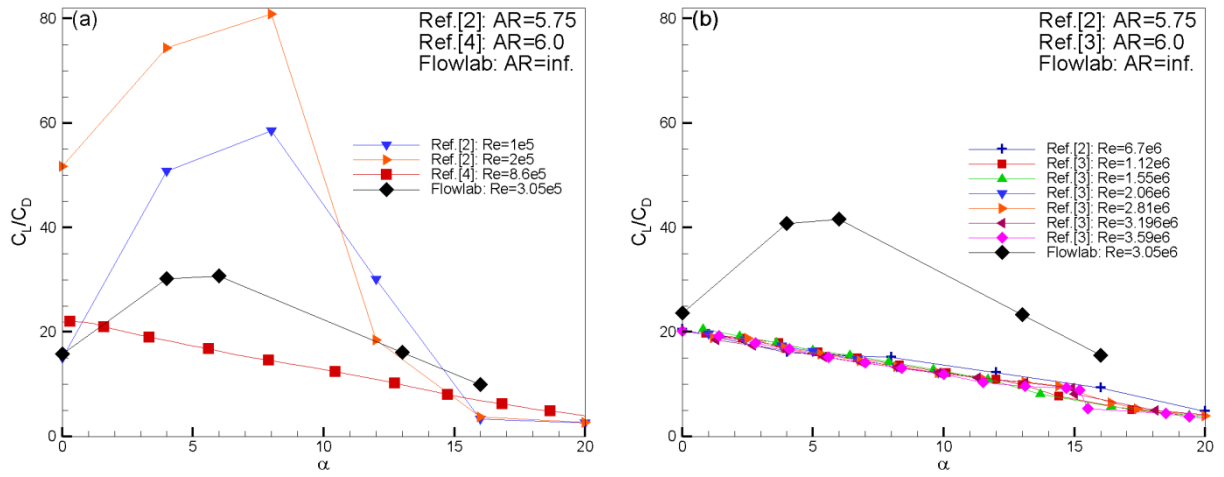


Fig. 17  $C_D$  vs  $\alpha$  with largest AR, Flowlab solutions added: (a)  $Re=O(10^5)$ , (b)  $Re=O(10^6)$

4.3  $C_p$  with largest AR

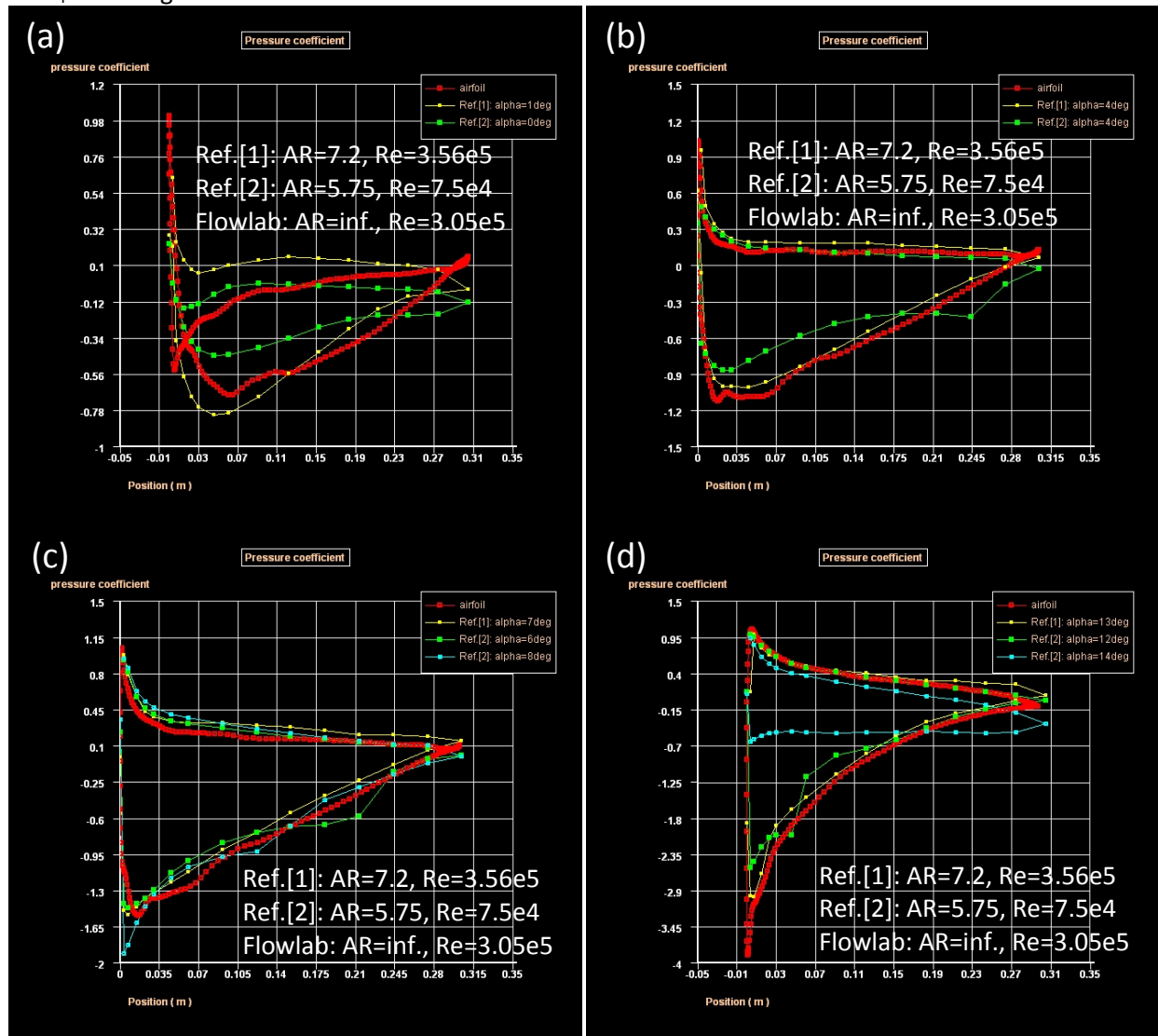


Fig. 18  $C_p$  distribution with largest AR, Flowlab solutions added  
 (a)  $\alpha \approx 0^\circ$ , (b)  $\alpha \approx 4^\circ$ , (c)  $\alpha \approx 7^\circ$ , (d)  $\alpha \approx 13^\circ$

5. Comparison between EFD benchmark data and IIHR experimental data

5.1  $C_L$  vs  $\alpha$

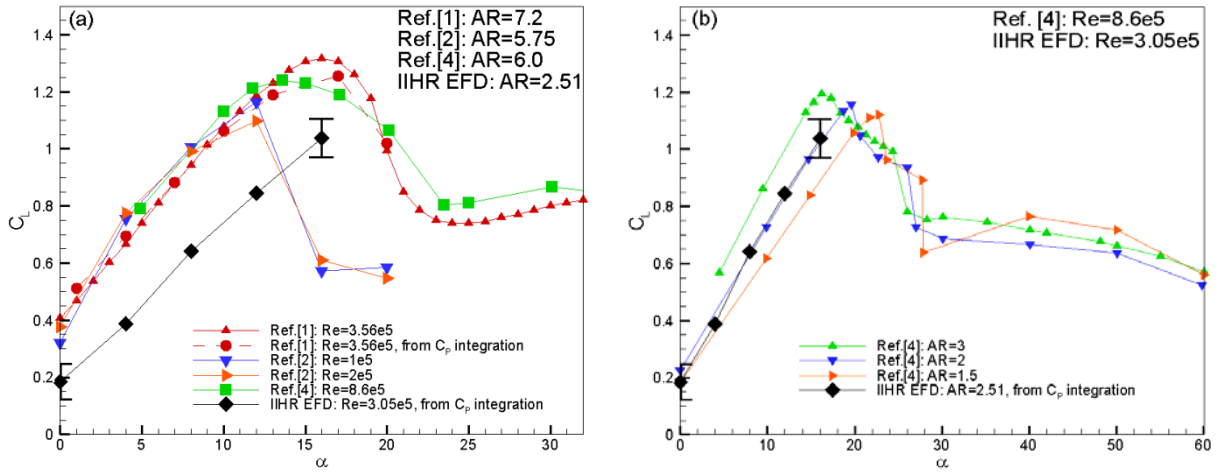


Fig. 19  $C_L$  vs  $\alpha$ , IIHR EFD data added: (a) large AR ( $\geq 5.75$ ), (b) small AR ( $1.5 \leq AR \leq 3$ )

5.2  $C_p$

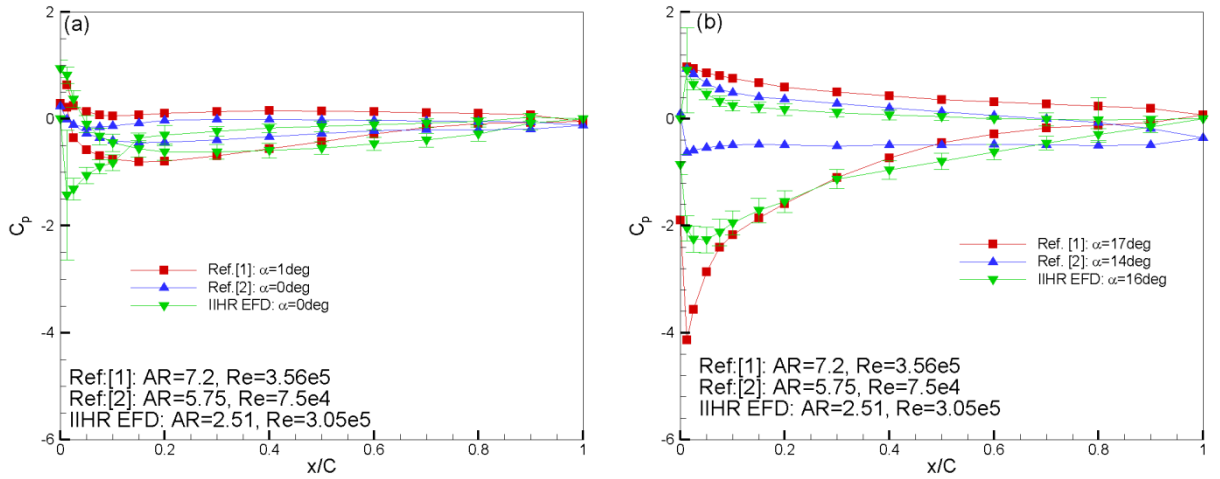


Fig. 20  $C_p$  distribution, IIHR EFD data added: (a)  $\alpha \approx 0$ deg, (b)  $\alpha \approx 16$ deg

6. Comparison between EFD benchmark data, IIHR experimental data and Flowlab solution

6.1  $C_L$  vs  $\alpha$

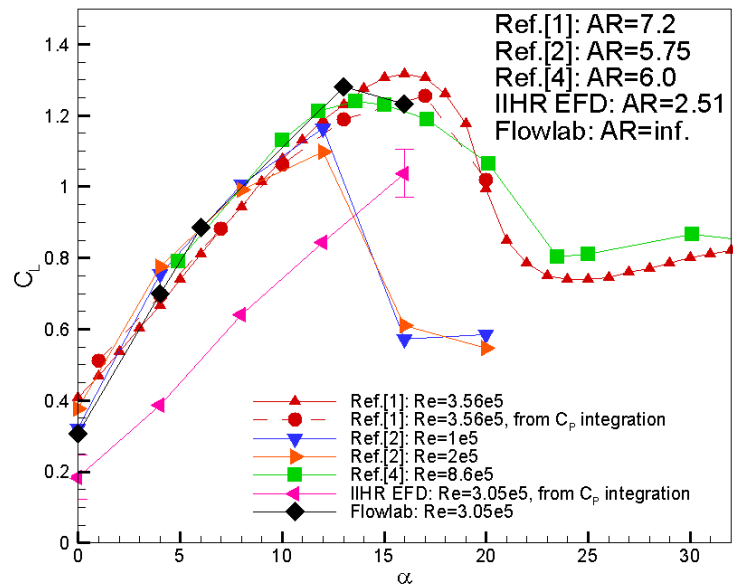


Fig. 21  $C_L$  vs  $\alpha$

6.2  $C_p$

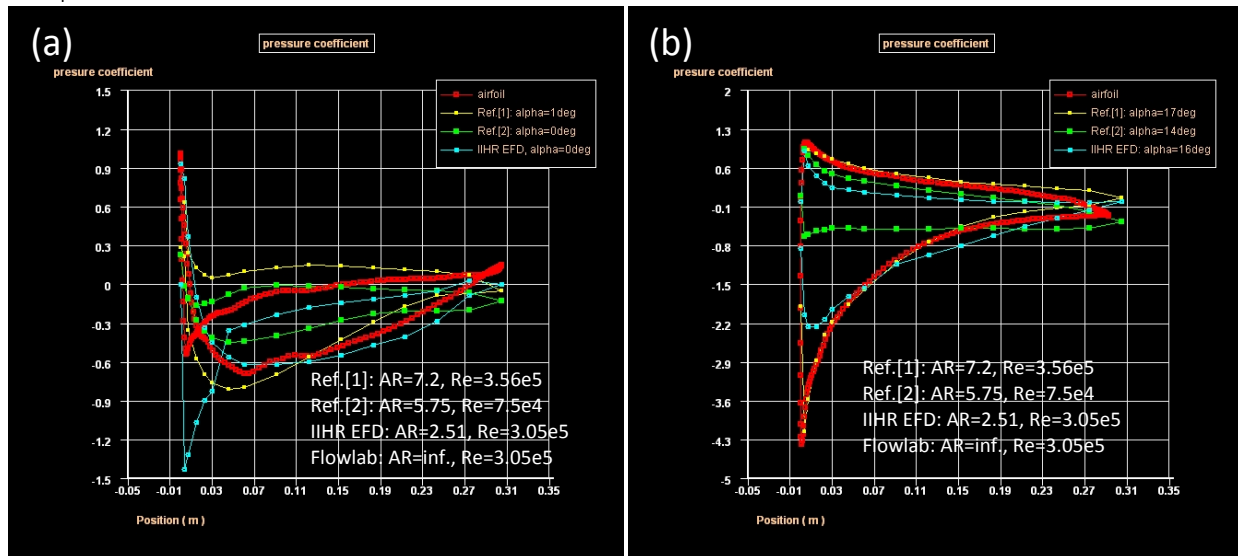


Fig. 22  $C_p$  distribution: (a)  $\alpha \approx 0\text{deg}$ , (b)  $\alpha \approx 16\text{deg}$

7. Discussion and Conclusion (To be added.)